Supplemental Information

Age model update for ODP Sites 1090 and 806

At ODP Site 1090, following initial publication of the SST data (Martinez-Garcia et al., 2010) an alternative orbitally-tuned age model was generated using *n*-alkane concentrations as a proxy for dust inputs, and an anticipated continuation of the Pleistocene relationship of high dust with high δ^{18}O i.e. during glacial stages (Martinez-Garcia et al., 2011). This *n*-alkane age model aligns KM5c with high *n*-alkane concentrations and low SSTs, whereas the reverse pattern might be expected (Figure S1). If the cold interval is re-aligned to KM4, SSTs during KM5c at ODP 1090 are elevated by 0.5°C (Figure S1). Given current stratigraphic information for ODP 1090 it is not possible to determine which of these scenarios is correct; thus, we present the SST anomalies according to the original age model, noting that there could be an additional increase in those anomalies of up to 0.5°C depending upon the choice of sample ages.

At ODP Site 806, uncertainty over age control resulted from the absence of an agreed splice across the multiple holes drilled by ODP. High-resolution benthic foraminifera δ^{18}O records were generated on Hole 806B (Bickert et al., 1993;Karas et al., 2009). Here we update the age model using the HMM-Stack Matlab code (Lin et al., 2014), which aligns to the Prob-stack (Ahn et al., 2017). Additionally, we created a modified meters composite depth (mcd). Using the depth scale generated by Karas et al., (2009) to account for core expansion, we amend Holes 806A and 806C to this depth scale (*Matlab code will be provided*). The KM5c interval is muted in Prob-stack in comparison to LR04 (Ahn et al., 2017). Given the variability in the Site 806 benthic δ^{18}O record (Figure 1), it is difficult to identify the KM5c interval and we rely on the probabilistic alignment of HMM-Match. If we tied the record to LR04 between M2 and KM2 and assumed a linear sedimentation rate, however, the age model in practice would be similar.

Alkenone calibrations

The majority of the alkenone-derived sea-surface temperature (SST) datasets included in the PlioVAR synthesis used the U^{K}_{37}' index, and applied the core-top calibration (60°S–60°N) by Müller et al. (1998) (hereafter Müller98; Tables S2 and S3). Several PlioVAR datasets were originally published using the laboratory culture calibration of *Emiliania huxleyi* by Prahl et al. (1988) (Table S3); these data were converted to Müller98 so that all sites used the same linear global calibration. The Bayesian U^{K}_{37}' calibration (BAYSPLINE) was then applied to all sites. Whilst the Müller98 calibration indicates mean annual SSTs for high latitudes, at sites >45°N (Pacific) and >48°N (Atlantic), and in the Mediterranean Sea, BAYSPLINE explicitly reconstructs seasonal SST (Tierney and Tingley, 2018).

Table S3 and Figure S2 compare the reconstructed SST anomalies for KM5c (relative to pre-industrial) for the 23 sites which provided alkenone data. In the mid- and high-latitudes, Müller98 tends to generate warmer SSTs compared to BAYSPLINE, with the difference ≤0.9 °C (Table S3). There is relatively little variability in the offset (± 0.15 °C) although that may reflect low sample numbers for some sites (Figure S2). In the low latitudes, where SSTs exceed ~24.5°C (applying Müller98), the non-linearity of the BAYSPLINE calibration has its biggest impact (Figure S2). For most low-latitude sites SSTs are ~1°C warmer using BAYSPLINE, but the difference can be as high as 1.67 °C ± 0.01°C (ODP 1143). The warmer low-latitudes in BAYSPLINE reduce the meridional T gradient, but both Müller98 and BAYSPLINE are consistent in showing enhanced warming at mid- and high-latitudes.

Foraminifera Mg/Ca calibrations

A range of foraminifera species, Mg/Ca-SST calibrations, and corrections for non-thermal impacts on Mg/Ca had been employed for the original published data (Table S4). We present the data as published, recognising the choices made by the original researchers in identifying the best approach for their site. The Bayesian calibration, BAYMAG, was then applied to all data following the settings detailed in the Methods.

Table S4 and Figure S3 compared the reconstructed SST anomalies for KM5c (relative to pre-industrial) for the 12 sites which provided foraminifera Mg/Ca data. A wide range of offsets is recorded, both positive and negative, and there is no clear pattern in terms of latitude or species.

Table S1. Sites used in the PlioVAR synthesis, their age constraints and SST proxies, can be accessed at https://pliovar.github.io/km5c.html.

Table S2. Alkenone indices and temperature calibrations discussed in the text. [$C_{37:x}$] refers to the concentration of the C_{37} alkenone with x unsaturations.

Alkenone index	**Calibration to ocean temperature**	**Sample type; Interpretation**	**Calibration reference**
U^{K}_{37}' = [$C_{37:2}$] / ([$C_{37:2}$] + [$C_{37:3}$])	U^{K}_{37}' = 0.034T + 0.039	*Emiliania huxleyi* cultures; Growth temperature	Prahl et al. (1998)
U^{K}_{37}' (as above)	U^{K}_{37}' = 0.033T + 0.044	Core tops, 60°S to 60°N; Mean annual SST	Muller et al. (1998)
U^{K}_{37}' (as above)	Bayesian calibration (BAYSPLINE)	Core tops, 60°S to 70°N Mean annual SST, except seasonal SST in high latitudes (>48°N) and Mediterranean	Tierney and Tingley (2018)

Table S3: The impact of applying two alkenone calibrations on the PlioVAR SST reconstructions for KM5c (3.195–3.215 Ma), sorted by basin and latitude (from N to S). All data were converted to the Muller et al. (1998) calibration prior to analysis. The recommended prior standard deviation scalar (pstd) of 10 was applied to all sites, excluding for high U^{K}_{37}' values where the more restrictive value of 5 was used, as recommended in the BAYSPLINE calibration (Tierney and Tingley, 2018).

Site	Original calibration	Original reference(s)	T difference (BAYSPLINE 50% level - Muller 98)
Atlantic Ocean and Mediterranean Sea			
907	Müller et al. (1998)	Herbert et al. (2016)	- 0.34 °C (*n* = 1)
642	Müller et al. (1998)	Bachem et al. (2016)	- 0.66 °C ± 0.02 °C
982	Prahl et al. (1998)	Herbert et al. (2016), Lawrence et al. (2009)	- 0.70 °C ± 0.01 °C
1313	Müller et al. (1998)	Naafs et al. (2010)	- 0.74 °C ± 0.01 °C
607	Prahl et al. (1998)	Lawrence et al. (2010)	- 0.74 °C ± 0.02 °C
999	Müller et al. (1998) Sonzogni et al. (1997)	Badger et al. (2013) Seki et al. (2010)	+ 0.87 °C ± 0.16 °C *(BAYSPLINE pstd = 5)*
662	Müller et al. (1998)	Herbert et al. (2010)	+1.25 °C ± 0.08 °C *(BAYSPLINE pstd=5)*
1387	Müller et al. (1998)	Tzanova & Herbert (2015)	+0.34 °C ± 0.28 °C *(BAYSPLINE pstd=5)*
Punto Piccola	Müller et al. (1998)	Herbert et al. (2015)	-0.19 °C ± 0.08 °C *(BAYSPLINE pstd=5)*
609	Müller et al. (1998)	Lawrence and Woodard (2017)	-0.71 °C ± 0.02 °C
625	Müller et al. (1998)	Van der Weijst and Peterse (unpublished)	+0.92 °C ± 0.16 °C *(BAYSPLINE pstd=5)*
1081	Müller et al. (1998)	Rosell-Mele et al. (2014)	-0.47 °C (*n* = 1)
1082	Müller et al. (1998)	Etourneau et al. (2009)	-0.19 °C ± 0.15 °C
1084	Müller et al. (1998)	Rosell-Mele et al. (2014)	-0.51 °C ± 0.07 °C
1087	Müller et al. (1998)	Petrick et al. (2015)	-0.86 °C ± 0.01 °C
1090	Müller et al. (1998)	Martinez-Garcia et al. (2011;2010)	-0.39 °C ± 0.01 °C
Pacific Ocean			
1143	Müller et al. (1998)	Li et al. (2011)	+1.67 °C ± 0.01 °C *(BAYSPLINE pstd=5)*
1417	Müller et al. (1998)	Sanchez-Montes et al. (2019)	-0.59 °C (*n* = 1)
846	Müller et al. (1998)	Lawrence et al. (2006)	-0.23 °C ± 0.09 °C *(BAYSPLINE pstd=5)*
1337	Müller et al. (1998)	Li et al. (2019)	+1.65 °C (*n* = 1)
593	Müller et al. (1998)	McClymont et al. (2016)	-0.70 °C ± 0.02 °C
594	Müller et al. (1998)	Cabellero-Gill et al. (2019)	-0.64 °C ± 0.01 °C
1125	Müller et al. (1998)	Cabellero-Gill et al. (2019)	-0.74 °C ± 0.01 °C
Indian Ocean			
722	Müller et al. (1998)	Herbert et al. (2010)	+0.91 °C ± 0.08 °C

			(BAYSPLINE pstd=5)

Table S4: Comparison of published Mg/Ca calibration and BAYMAG for PlioVAR SST reconstructions for KM5c (3.195–3.215 Ma), sorted by basin and latitude (from N to S). The original Mg/Ca SST calibrations (and any corrections) used in the published datasets are shown.

Site	**Species**	**Original calibration**	**Original reference(s)**	**T difference (BAYMAG – published calibration)**
Atlantic Ocean				
609	*G. bulloides*	Mashiotta et al. (1999)	Bartoli et al. (2005)	+0.80 °C ± 0.83 °C
U1313	*G. bulloides*	Elderfield and Ganssen (2000)	Hennissen et al. (2014)	+4.75 °C ± 0.23 °C
603	*G. bulloides*	Elderfield and Ganssen (2000)	De Schepper et al. (2009)	+4.73 °C ± 0.74 °C
999	*T. sacculifer*	Nürnberg et al. (2000)	De Schepper et al. (2013)	-0.47 °C ± 0.09 °C
959	*T. sacculifer*	Dekens et al. (2002) with Evans et al. (2016) Mg/Ca_{sw} correction	Van der Weijst and Peterse (unpublished)	-4.12 °C ± 0.24 °C
516	*T. sacculifer*	Anand et al. (2003)	Karas et al., (2017)	+1.26 °C ± 0.24 °C
Pacific Ocean				
1143	*G. ruber*	Dekens et al. (2002)	Tian et al., (2006)	-0.57 °C ± 0.17 °C
1241	*T. sacculifer*	Nürnberg et al. (2000)	Groeneveld et al. (2006)	+2.73 °C ± 0.37 °C
806	*T. sacculifer*	Dekens et al. (2002)	Wara et al. (2005)	+1.46 °C ± 0.04 °C
Indian Ocean				
709	*T. sacculifer*	Anand et al. (2003) with Regenberg et al. (2006) correction	Karas et al. (2011)	+0.29 °C (n = 1)
214	*T. sacculifer*	Anand et al. (2003) with Regenberg et al. (2006) correction	Karas et al. (2009)	-1.05 °C (n = 1)
763	*T. sacculifer*	Anand et al. (2003) with Regenberg et al. (2006) correction	Karas et al. (2011)	+1.34 °C (n = 1)

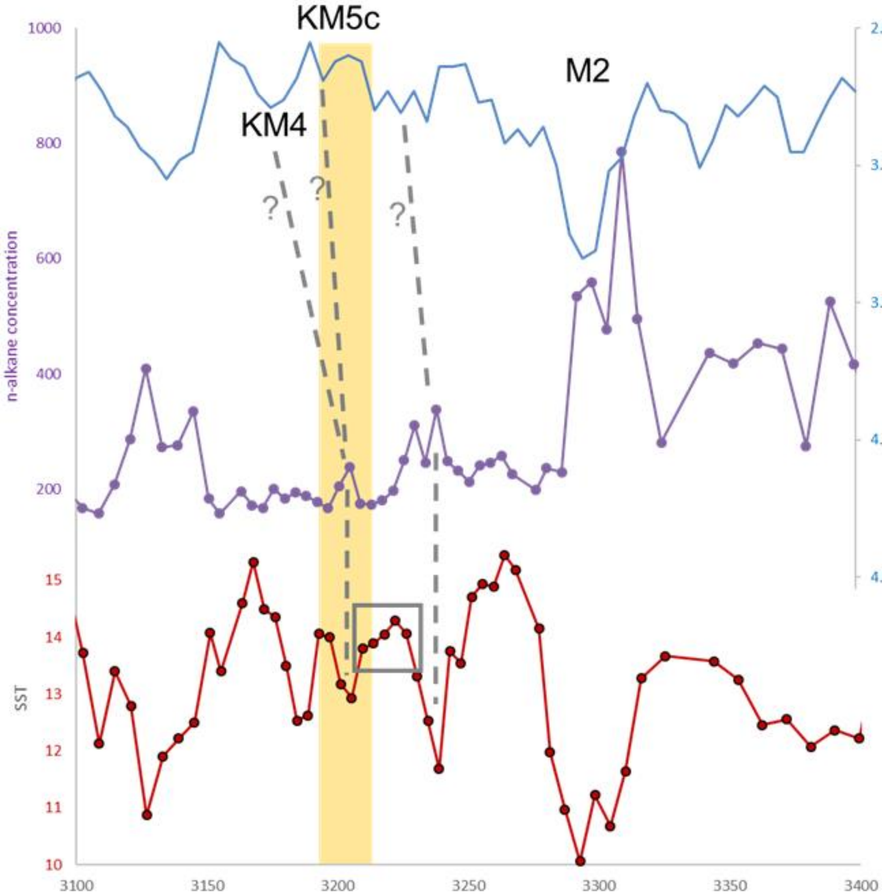

Figure S1: Age control for ODP 1090. *n*-Alkane concentrations and SSTs plotted on the original age scale of Martinez-Garcia et al. (2011), whereby the Pleistocene relationship of high *n*-alkane concentrations during glacial stages was applied. The KM5c window adopted in the main text is indicated by the vertical yellow bar. An alternative alignment of the published KM5c *n*-alkane peak and SST minimum into KM4 or the final stages of KM5c (dashed lines) leads to an increase in KM5c SSTs of up to 0.5*C (grey box).

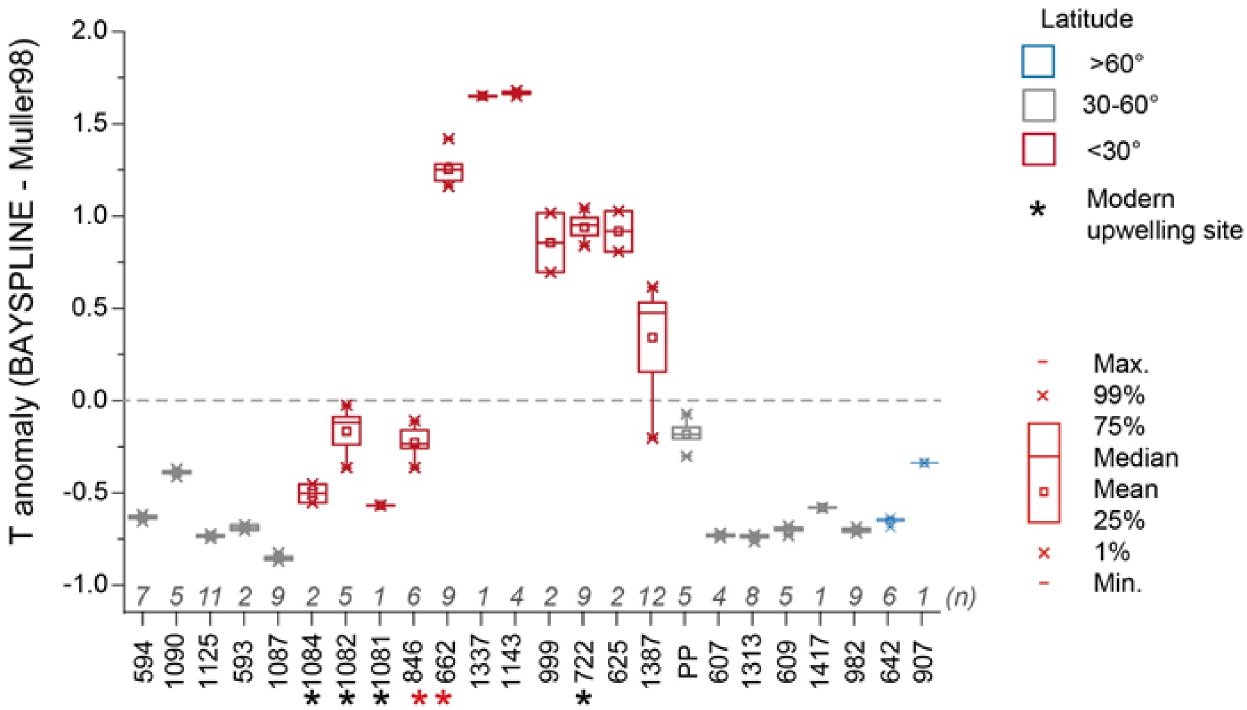

Figure S2: the impact of applying either the non-linear BAYSPLINE (Tierney and Tingley, 2018) or linear Muller et al. (1998) calibrations for the alkenone U^{K}_{37}' index for the KM5c interval. Temperature anomaly information is also provided in Table S3. Sites are ordered by latitude as shown in Figure 4 of the main text (594 at 46°S through to 907 at 69°N). Four sites contain only one data point for the KM5c interval (1081, 1337, 1417 and 907).

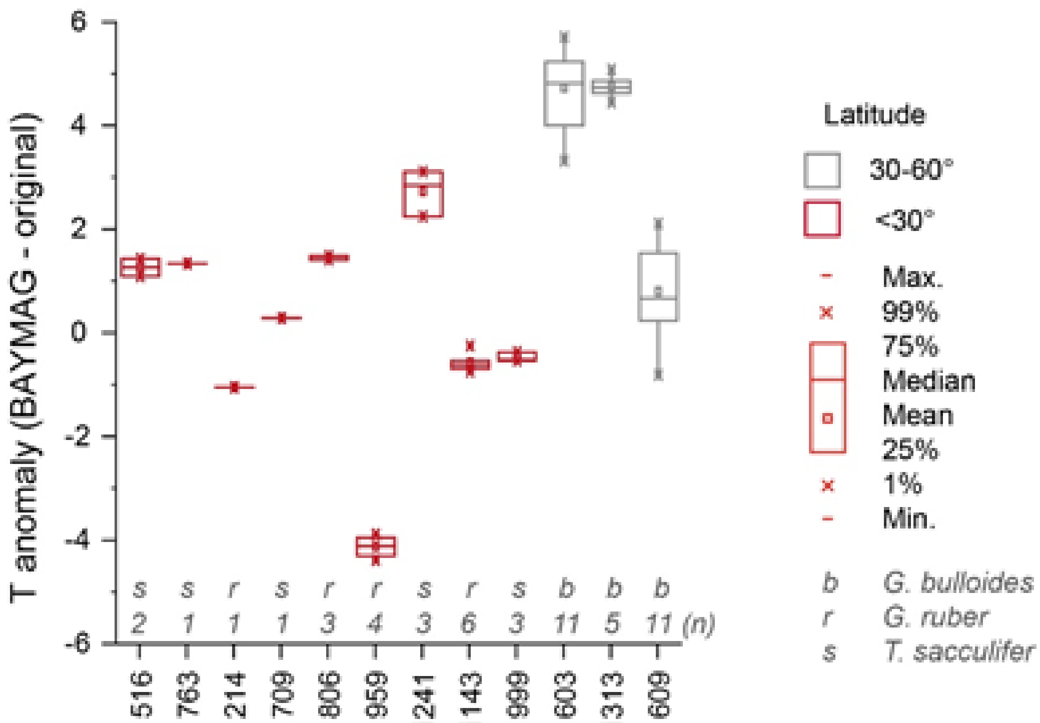

Figure S3: impact of applying BAYMAG to original (published) Mg/Ca temperature calibrations. Temperature anomaly information is provided in Table S4. Sites are ordered by latitude as shown in Figure 4
100 **of the main text (516 at -30°S to 609 at 50°N). Three sites contain only one data point for the KM5c interval (763, 214, 709).**

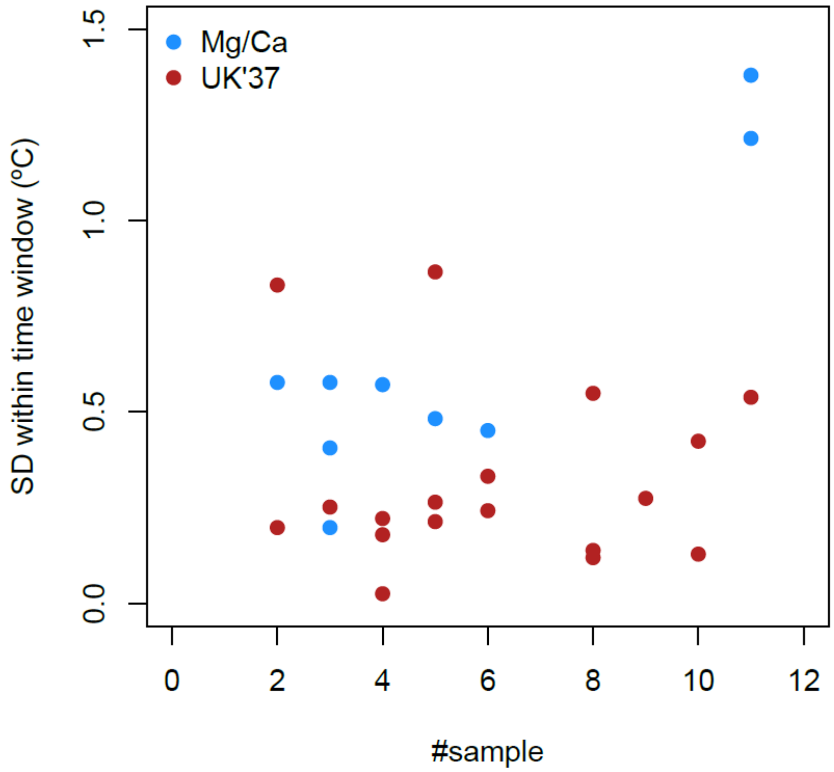

Figure S4: The impact of the numbers of data points within KM5c (#sample) on the temporal variability (standard deviation; SD). For most sites, SD is <1°C (and closer to 0-0.5 °C).

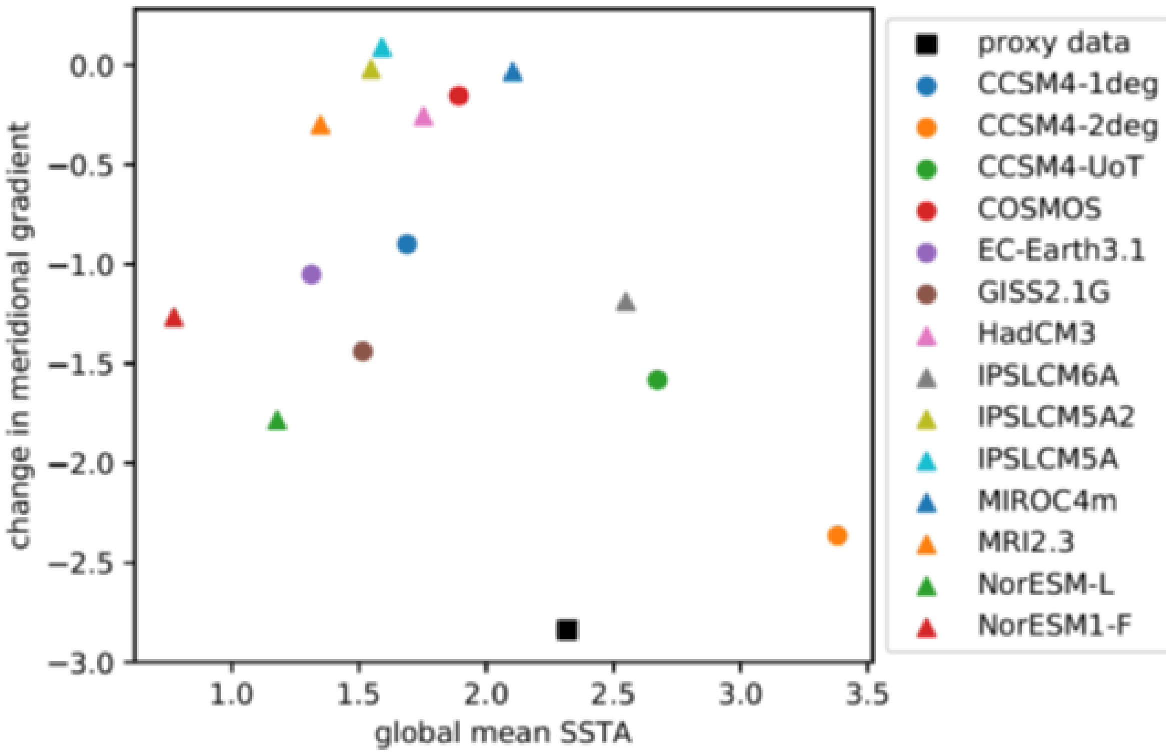

Figure S4: impact of changing high/low latitude bands on meridional SST gradient calculations. The high-latitude box is expanded from >60°N/S (Figure 3) to include sites between 45-60°N/S, and the low-latitude box is restricted to 15°S-15°N. This adds a further 4 sites to the original 2 included in the high-latitude box, and removes the possible influence of the Benguela upwelling sites from the low-latitude SST calculations, given data-model mismatch (Figure 4). Although there is minimal change in the proxy data meridional T gradient anomaly (2.8°C here compared to 2.6°C in Figure 2), the data no longer agree with the PlioMIP2 models.

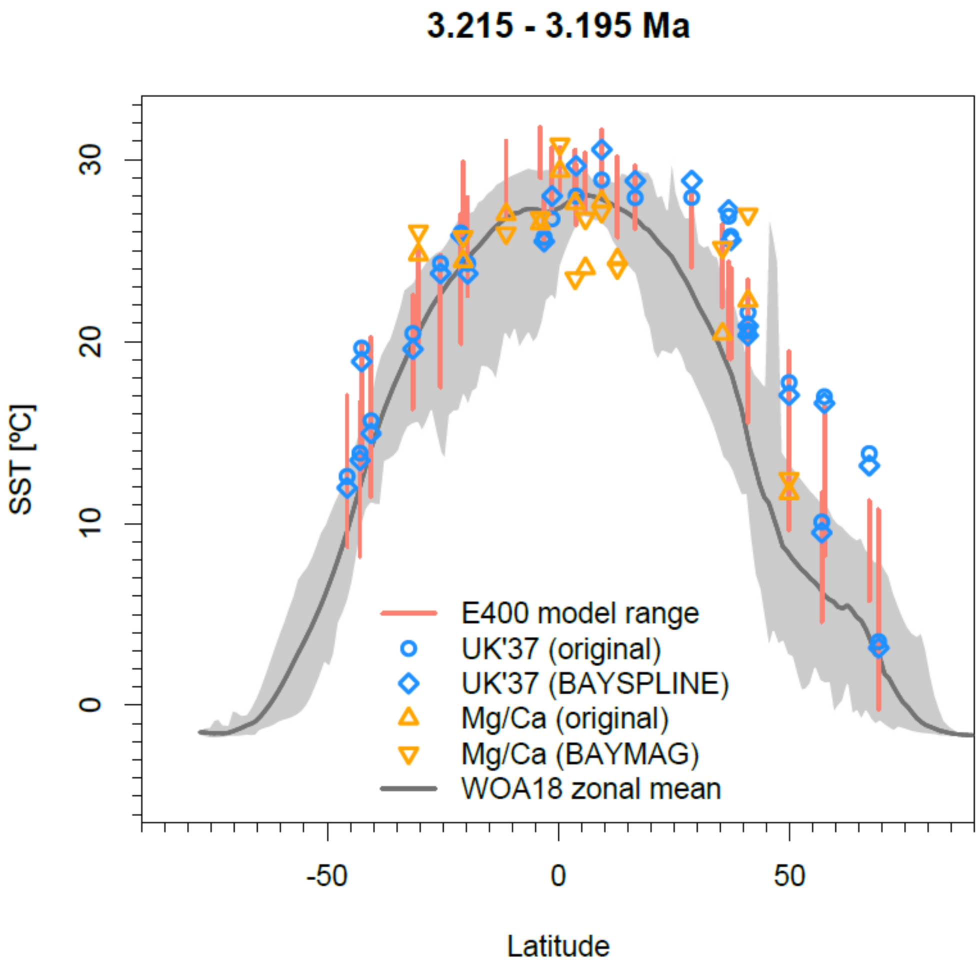

Figure S5: Absolute SSTs for each site, for modern (World Ocean Atlas, 2018 (Boyer et al., 2018)) and for KM5c (proxy data and models as for Figure 4).

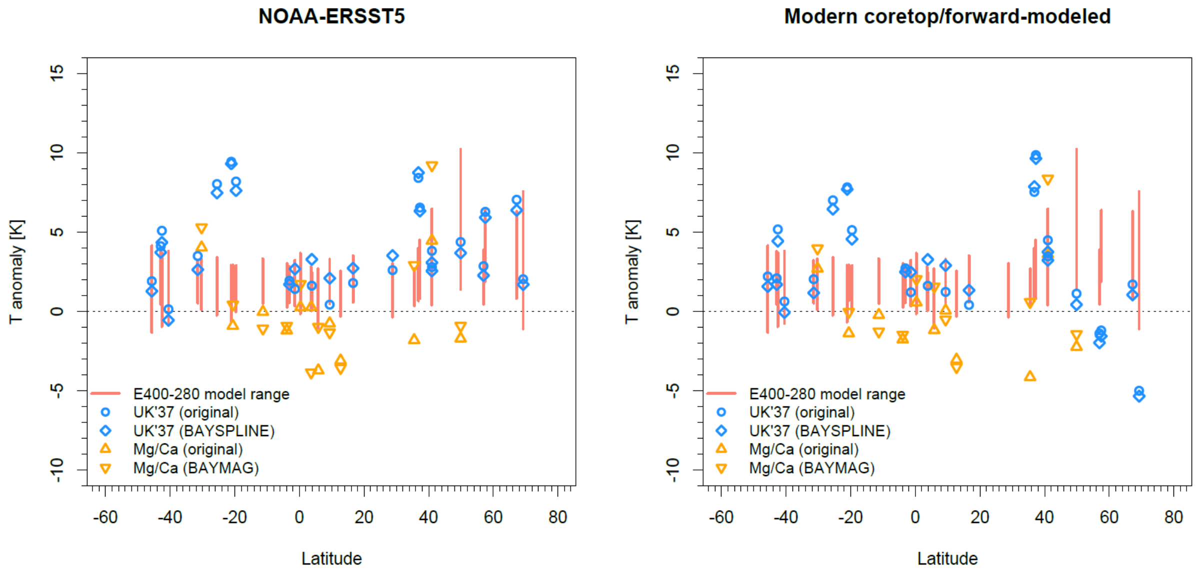

Figure S6: Impact of pre-industrial choice on the anomaly calculation. Left: ERSSTv5 (as shown in Figure 4 of the main text); right: the anomalies using the nearest available core-top data (for alkenones) and the forward-modelled 'core-top' from BAYMAG (Tierney et al., 2019), which uses World Ocean Atlas SST data (Locarnini et al., 2013). For site information see https://pliovar.github.io/km5c.html).

Supplement reference list

Ahn, S., Khider, D., Lisiecki, L. E., and Lawrence, C. E.: A probabilistic Pliocene–Pleistocene stack of benthic δ18O using a profile hidden Markov model, Dynamics and Statistics of the Climate System, 2, 10.1093/climsys/dzx002, 2017.

Anand, P., and Elderfield, H.: Calibration of Mg/Ca thermometry in planktonic foraminifera from a sediment trap time series, Paleoceanography, 18, 1050, doi:1010.1029/2002PA000846, 2003.

Bachem, P. E., Risebrobakken, B., and McClymont, E. L.: Sea surface temperature variability in the Norwegian Sea during the late Pliocene linked to subpolar gyre strength and radiative forcing, Earth and Planetary Science Letters, 446, 113-122, http://dx.doi.org/10.1016/j.epsl.2016.04.024, 2016.

Badger, M. P. S., Schmidt, D. N., Mackensen, A., and Pancost, R. D.: High resolution alkenone palaeobarometry indicates stable pCO_2 during the Pliocene (3.3 to 2.8 Ma), Proceedings of the Royal Society, A, 371, Article 20130094, 2013.

Bartoli, G., Sarnthein, M., Weinelt, M., Erlenkeuser, H., Garbe-Schönberg, D., and Lea, D. W.: Final closure of Panama and the onset of northern hemisphere glaciation, Earth and Planetary Science Letters, 237, 33-44, https://doi.org/10.1016/j.epsl.2005.06.020, 2005.

Bickert, T., Berger, W. H., Burke, S., Schmidt, H., and Wefer, G.: Late Quaternary stable isotope record of benthic foraminifers: Sites 805 and 806, Ontong Java Plateau, in: Proc. ODP, Sci. Results, 130, edited by: Berger, W. H., Kroenke, L. W., Mayer, L. A., and et al., College Station, TX (Ocean Drilling Program), 411–420. doi:410.2973/odp.proc.sr.2130.2025.1993, 1993.

Boyer, T. P., Baranova, O. K., Coleman, C., Garcia, H. E., Grodsky, A., Locarnini, R. A., Mishonov, A. V., O'Brien, T. D., Paver, C. R., Reagan, J. R., Seidov, D., Smolyar, I. V., Weathers, K., and Zweng, M. M.: World Ocean Database 2018, in preparation, https://www.nodc.noaa.gov/OC5/indprod.html, 2018.

Caballero-Gill, R. P., Herbert, T. D., and Dowsett, H. J.: 100-kyr Paced Climate Change in the Pliocene Warm Period, Southwest Pacific, Paleoceanography and Paleoclimatology, 34, 524-545, 10.1029/2018pa003496, 2019.

De Schepper, S., Head, M. J., and Groeneveld, J.: North Atlantic Current variability through marine isotope stage M2 (circa 3.3. Ma) during the mid-Pliocene, Paleoceanography, 24, PA4206, doi:4210.1029/2008PA001725, 2009.

De Schepper, S., Groeneveld, J., Naafs, B. D. A., Van Renterghem, C., Hennissen, J., Head, M. J., Louwye, S., and Fabian, K.: Northern Hemisphere Glaciation during the Globally Warm Early Late Pliocene, PLoS ONE, 8, e81508. doi:81510.81371/journal.pone.0081508, 2013.

Dekens, P. S., Lea, D. W., Pak, D. K., and Spero, H. J.: Core top calibration of Mg/Ca in tropical foraminifera: Refining paleotemperature estimation, Geochemistry Geophysics Geosystems, 3, 1022, doi:1010.1029/2001GC000200. , 2002.

Elderfield, H., and Ganssen, G.: Past temperature and δ18O of surface ocean waters inferred from foraminiferal Mg/Ca ratios, Nature, 405, 442-445, 10.1038/35013033, 2000.

Etourneau, J., Martinez, P., Blanz, T., and Schneider, R.: Pliocene-Pleistocene variability of upwelling activity, productivity, and nutrient cycling in the Benguela region, Geology, 37, 871-874, 10.1130/g25733a.1, 2009.

Evans, D., Brierley, C., Raymo, M. E., Erez, J., and Müller, W.: Planktic foraminifera shell chemistry response to seawater chemistry: Pliocene–Pleistocene seawater Mg/Ca, temperature and sea level change, Earth and Planetary Science Letters, 438, 139-148, https://doi.org/10.1016/j.epsl.2016.01.013, 2016.

Groeneveld, J., Steph, S., Tiedemann, R., Garbe-Schönberg, C., Nürnberg, D., and Sturm, A.: Pliocene mixed-layer oceanography for Site 1241, using combined Mg/Ca and $\delta^{18}O$ analyses of Globigerinoides sacculifer, Proceedings of the Ocean Drilling Program: Scientific Results, 202, 1-27, 2006.

Hennissen, J. A. I., Head, M. J., De Schepper, S., and Groeneveld, J.: Palynological evidence for a southward shift of the North Atlantic Current at ~2.6 Ma during the intensification of late Cenozoic Northern Hemisphere glaciation, Paleoceanography, 29, 564-580, 10.1002/2013pa002543, 2014.

Herbert, T. D., Peterson, L. C., Lawrence, K. T., and Liu, Z.: Tropical Ocean Temperatures Over the Past 3.5 Million Years, Science, 328, 1530-1534, 10.1126/science.1185435, 2010.

Herbert, T. D., Ng, G., and Cleaveland Peterson, L.: Evolution of Mediterranean sea surface temperatures 3.5–1.5 Ma: Regional and hemispheric influences, Earth and Planetary Science Letters, 409, 307-318, http://dx.doi.org/10.1016/j.epsl.2014.10.006, 2015.

Herbert, T. D., Lawrence, K. T., Tzanova, A., Peterson, L. C., Caballero-Gill, R., and Kelly, C. S.: Late Miocene global cooling and the rise of modern ecosystems, Nature Geoscience, 9, 843-847, doi:810.1038/ngeo2813, 2016.

Karas, C., Nurnberg, D., Gupta, A. K., Tiedemann, R., Mohan, K., and Bickert, T.: Mid-Pliocene climate change amplified by a switch in Indonesian subsurface throughflow, Nature Geoscience, 2, 434-438, http://www.nature.com/ngeo/journal/v2/n6/suppinfo/ngeo520_S1.html, 2009.

Karas, C., Nürnberg, D., Tiedemann, R., and Garbe-Schönberg, D.: Pliocene Indonesian Throughflow and Leeuwin Current dynamics: Implications for Indian Ocean polar heat flux, Paleoceanography, 26, PA2217, 10.1029/2010pa001949, 2011.

Karas, C., Nürnberg, D., Bahr, A., Groeneveld, J., Herrle, J. O., Tiedemann, R., and deMenocal, P. B.: Pliocene oceanic seaways and global climate, Scientific Reports, 7, 39842, 10.1038/srep39842, 2017.

Lawrence, K. T., Liu, Z., and Herbert, T. D.: Evolution of the Eastern Tropical Pacific Through Plio-Pleistocene Glaciation, Science, 312, 79-83, 2006.

Lawrence, K. T., Herbert, T. D., Brown, C. M., Raymo, M. E., and Haywood, A. M.: High-amplitude variations in North Atlantic sea surface temperature during the early Pliocene warm period, Paleoceanography, 24, 2009.

Lawrence, K. T., Sosdian, S., White, H. E., and Rosenthal, Y.: North Atlantic climate evolution through the Plio-Pleistocene climate transitions, Earth and Planetary Science Letters, 300, 329-342, https://doi.org/10.1016/j.epsl.2010.10.013, 2010.

Lawrence, K. T., and Woodard, S. C.: Past sea surface temperatures as measured by different proxies—A cautionary tale from the late Pliocene, Paleoceanography, 32, 318-324, 10.1002/2017pa003101, 2017.

Li, L., Li, Q., Tian, J., Wang, P., Wang, H., and Liu, Z.: A 4-Ma record of thermal evolution in the tropical western Pacific and its implications on climate change, Earth and Planetary Science Letters, 309, 10-20, 2011.

Lin, L., Khider, D., Lisiecki, L. E., and Lawrence, C. E.: Probabilistic sequence alignment of stratigraphic records, Paleoceanography, 29, 976–989, 2014.

Liu, J., Tian, J., Liu, Z., Herbert, T. D., Fedorov, A. V., and Lyle, M.: Eastern equatorial Pacific cold tongue evolution since the late Miocene linked to extratropical climate, Science Advances, 5, eaau6060, 10.1126/sciadv.aau6060, 2019.

Martinez-Garcia, A., Rosell-Mele, A., McClymont, E. L., Gersonde, R., and Haug, G. H.: Subpolar Link to the Emergence of the Modern Equatorial Pacific Cold Tongue, Science, 328, 1550-1553, 10.1126/science.1184480, 2010.

Martinez-Garcia, A., Rosell-Mele, A., Jaccard, S. L., Geibert, W., Sigman, D. M., and Haug, G. H.: Southern Ocean dust-climate coupling over the past four million years, Nature, 476, 312-315, 2011.

Mashiotta, T. A., Lea, D. W., and Spero, H. J.: Glacial–interglacial changes in Subantarctic sea surface temperature and δ18O-water using foraminiferal Mg, Earth and Planetary Science Letters, 170, 417-432, https://doi.org/10.1016/S0012-821X(99)00116-8, 1999.

McClymont, E. L., Elmore, A. C., Kender, S., Leng, M. J., Greaves, M., and Elderfield, H.: Pliocene-Pleistocene evolution of sea surface and intermediate water temperatures from the Southwest Pacific, Paleoceanography, PA002954, 2016.

Müller, P. J., Kirst, G., Ruhland, G., Storch, I. V., and Rosell-Melé, A.: Calibration of the alkenone paleotemperature index U^{k}_{37}' based on core-tops from the eastern South Atlantic and the global ocean (60°N–60°S), Geochimica et Cosmochimica Acta, 62, 1757–1772, 1998.

Naafs, B. D. A., Stein, R., Hefter, J., Khélifi, N., De Schepper, S., and Haug, G. H.: Late Pliocene changes in the North Atlantic Current, Earth and Planetary Science Letters, 298, 434-442, http://dx.doi.org/10.1016/j.epsl.2010.08.023, 2010.

Nürnberg, D., Müller, A., and Schneider, R. R.: Paleo-sea surface temperature calculations in the equatorial east Atlantic from Mg/Ca ratios in planktic foraminifera: A comparison to sea surface temperature estimates from U37K′, oxygen isotopes, and foraminiferal transfer function, Paleoceanography, 15, 124-134, 10.1029/1999pa000370, 2000.

Petrick, B., McClymont, E. L., Felder, S., Rueda, G., Leng, M. J., and Rosell-Melé, A.: Late Pliocene upwelling in the Southern Benguela region, Palaeogeography, Palaeoclimatology, Palaeoecology, 429, 62-71, http://dx.doi.org/10.1016/j.palaeo.2015.03.042, 2015.

Prahl, F. G., Muehlhausen, L. A., and Zahnle, D. I.: Further evaluation of long-chain alkenones as indicators of paleoceanographic conditions, Geochimica et Cosmochimica Acta, 52, 2303-2310, 1988.

Regenberg, M., Nürnberg, D., Steph, S., Groeneveld, J., Garbe-Schönberg, D., Tiedemann, R., and Dullo, W.-C.: Assessing the effect of dissolution on planktonic foraminiferal Mg/Ca ratios: Evidence from Caribbean core tops, Geochemistry Geophysics Geosystems, 7, Q07P15, doi:10.1029/2005GC001019, 2006.

Rosell-Melé, A., Martínez-Garcia, A., and McClymont, E. L.: Persistent warmth across the Benguela upwelling system during the Pliocene epoch, Earth and Planetary Science Letters, 386, 10-20, http://dx.doi.org/10.1016/j.epsl.2013.10.041, 2014.

Sánchez-Montes, M. L., McClymont, E. L., Lloyd, J. M., Müller, J., Cowan, E. A., and Zorzi, C.: Late Pliocene Cordilleran Ice Sheet development with warm Northeast Pacific sea surface temperatures, Clim. Past Discuss. (accepted), 2019, 1-23, 10.5194/cp-2019-29, 2019.

Seki, O., Foster, G. L., Schmidt, D. N., Mackensen, A., Kawamura, K., and Pancost, R. D.: Alkenone and boron-based Pliocene pCO2 records, Earth and Planetary Science Letters, 292, 201-211, 2010.

Tian, J., Pak, D. K., Wang, P., Lea, D., Cheng, X., and Zhao, Q.: Late Pliocene monsoon linkage in the tropical South China Sea, Earth and Planetary Science Letters, 252, 72-81, https://doi.org/10.1016/j.epsl.2006.09.028, 2006.

Tierney, J. E., and Tingley, M. P.: BAYSPLINE: A New Calibration for the Alkenone Paleothermometer, 33, 281-301, 10.1002/2017pa003201, 2018.

Tierney, J. E., Malevich, S. B., Gray, W., Vetter, L., and Thirumalai, K.: Bayesian calibration of the Mg/Ca paleothermometer in planktic foraminifera, Paleoceanography and Paleoclimatology, 31, https://doi.org/10.1029/2019PA003744, 10.1029/2019pa003744, 2019.

Tzanova, A., and Herbert, T. D.: Regional and global significance of Pliocene sea surface temperatures from the Gulf of Cadiz (Site U1387) and the Mediterranean, Global and Planetary Change, 133, 371-377, https://doi.org/10.1016/j.gloplacha.2015.07.001, 2015.

Wara, M. W., Ravelo, A. C., and Delaney, M. L.: Permanent El Nino-Like Conditions During the Pliocene Warm Period, Science, 309, 758-761, 2005.